NATIONAL TRANSPORTATION SAFETY BOARD
Office of Research and Engineering
Materials Laboratory Division
Washington, D.C. 20594

January 27, 2011

MATERIALS LABORATORY FACTUAL REPORT Report No. 11-001

A. INVESTIGATION INFORMATION

Place	:	Miami, Florida
Date	:	October 26, 2010
Vehicle	:	Boeing 757-223, N626AA
NTSB No.	:	DCA11FA004
Investigator	:	Clinton Crookshanks, AS-40

B. COMPONENTS EXAMINED

Section of Fuselage Crown Skin.

C. DETAILS OF THE EXAMINATION

On October 26, 2010, about 9:30 pm eastern daylight time (EDT), an American Airlines Boeing 757-223, N626AA[1], operating as flight 1640 from Miami International Airport (MIA), Miami, Florida, to Boston Logan International Airport (BOS), Boston, Massachusetts, experienced a rapid decompression at 31,000 feet. The airplane had accumulated 22,450 cycles in 63,010 hours of service.

The airplane, shown in figure 1, was initially examined on October 28, 2010 in conjunction with the NTSB Structures Group. As shown, the fuselage skin had flapped open above and aft of the forward left (L1) entry door.

The affected fuselage panel was reportedly manufactured from 0.063 inch nominal thickness Alclad[2] 2024 T-3 aluminum alloy sheet[3]. The interior of the panel was chemically milled[4] into a waffle pattern of thinner (0.040 inch nominal) pockets circumferentially separated by full thickness tear straps and longitudinally by full thickness stringer pads. The thinner pockets transition into the thicker surrounding material at a single radiused step, referred to as a "chem-mill step" or fillet.

[1] N626AA is serial number 24584, Boeing line number 304, manufactured August 14, 1990.
[2] Alclad- Thin layers of pure aluminum are clad onto high strength aluminum sheet for enhanced corrosion resistance.
[3] QQ-A-250/5 Aluminum Alloy 2024, Plate and Sheet.
[4] Chemical milling is a process where selected material is removed through the chemical action of either strong acids or bases. Masking is applied to areas not being milled and the exposed areas are milled.

The milled panel forms a portion of the crown skin of the fuselage and extends from lap joints at stringer 4 on the left side (S-4L)[5] to lap joint at stringer 4 on the right side (S-4R) and from the butt joint at body station (BS) 439[6] forward to a butt joint at BS 297, as illustrated at the top of figure 2 with another drawing showing the internal arrangement of pockets in the aft portion of the panel below. A line drawing showing the interior features of the aft left portion of the panel are shown overlaid onto an image of the aircraft in the lower view of figure 3.

The flapped skin area was contained in the crown skin section between the stringer 4 left (S-4L) lap joint and stringer 3 left (S-3L), circumferentially and between tear straps located at body station (BS) 395 and 418 longitudinally, as shown in figure 3. The flap was wholly contained within the pocket of the 2nd fuselage bay forward of the butt joint at BS 439. The hole produced by the flap measured approximately 7 inches circumferentially and 18 inches longitudinally and generally followed the chemical milled steps just above the S-4L lap joint and the forward edge of the tear strap at the aft stringer. As examined, the forward 13 inched of the skin flap was bent outward (up) about 90 degrees along the lower chem-mill step at the S-3L pad. Abrasion marks on the forward edge of the flapped skin matched abrasions on the skin area above S-3L indicative of contact between the two areas. The aft 5 inches of the flap was fractured off and not recovered.

During initial visual inspections a longitudinal through-the-skin crack was uncovered between body stations 386 and 387 in the fuselage bay forward of the bay containing the flap. The crack location was highlighted by a faint smoky trail on the fuselage surface aft of the crack, as shown in figure 4. From the exterior, the crack appeared to coincide with the chemically milled radius above S-4L. Visually the crack was estimated to be approximately 1 3/16 inch long.

On-scene nondestructive inspection (NDI) of the panel using a sliding eddy current probe[7] uncovered an additional 1 inch long crack indication just forward of the thru crack approximately between BS 383 and 384.

A section of the skin panel from the S-4L lap joint to 2 rivets above S-3L and from 2 rivets forward of BS 377.7 (approximately BS 374.4) to the butt joint at BS 439 was removed from the airplane for examination in the NTSB Materials Laboratory. The removed area is indicated by the shaded red box in the upper image of figure 5 with the exterior and interior surfaces of the removed section shown below. The removed section fully included the 3 pocketed fuselage bays along the aft left edge of the skin panel. For the purposes of this report the bays will be referred to as the aft, middle and forward bays.

Initial examinations were conducted from October 26, 2010 through November 3, 2010 with representatives from Boeing, American Airlines, and FAA present.

[5] Stringers are numbered from the top centerline of the fuselage, designated stringer 1, and down the right and left sides of the fuselage (when viewed from the rear) and designated L or R to denote the appropriate side.
[6] Body stations are numbered from the front of the aircraft rearward and correspond to inch measurements along the fuselage.
[7] Boeing NDI personnel with the assistance of AA maintenance technicians performed the inspection.

Magnified optical inspections of the skin fracture surfaces at the edge of the hole in the middle bay, after partial cleaning revealed through-the-thickness fatigue cracking along most of the longitudinal chem-mill step just above the S-4L lap joint. Fatigue cracking was noted along 15 inches of the 18 inch long longitudinal fracture region, approximately from BS 400.5 to BS 416. Magnified examinations indicated a multitude of fatigue crack initiation points on the interior surface of the panel with progression outward through the thickness of the skin. Many of the fatigue crack origins were slightly offset circumferentially from adjacent origins producing many ratchet marks in the fatigue region as the individual fatigue crack front grew and merged, as shown in the upper view of figure 6. Complete penetration of the skin by fatigue cracking was observed on an approximate 2 ½ inch length of the fracture located between BS 412 and 415. The remaining fatigue region showed partial penetration of the skin by fatigue fracture with ductile overstress fracture accounting for the remaining skin thickness. Estimates of the amount of fatigue crack penetration of the skin at half inch intervals are depicted by the chart in figure 6.

Forward from the 100% penetration area, linked fatigue thumbnail cracks were found continuously at the inner surface up to about BS 408. From BS 408 to BS 403, the fatigue region became discontinuous with small regions of overstress fracture at the inner surface separating fatigue areas. Between BS 403 and the end of the fracture at BS 400.5, fatigue thumbnails were spotty and intermittent. Aft of the 100% area connected fatigue thumbnail cracks were present to the end of the fatigue region at about BS 416. At all locations, the fatigue propagation was through-the-thickness with no indications of purely longitudinal growth.

Features within the overstress fracture regions in the fatigue area indicated circumferential tensile yielding with no indications of longitudinal tearing except at the extreme ends near the circumferential portions of the flap. The fracture outside of the noted fatigue region was consistent with tearing overstress separation propagating away from S-4L.

The fatigue region was approximately in line with the chem-mill step that also paralleled the lap joint at stringer 4 left. Along the lap joint the step was initially visually obscured on the interior by sealant extruded from the lap joint, as shown in the upper view of figure 7. The sealant was removed from the chem-mill step and adjacent surfaces by scraping with wooden instruments after soaking in acetone. With the sealant removed the fatigue regions were located along the transition from the chem-mill step to the thinner pocket region, at approximately 0.035 to 0.050 inch from the full thickness region of the panel (see figure 7 lower view).

Magnified examination of the fatigue region revealed various amounts of post separation mechanical damage and through the thickness yielding. The inspections found that approximately between body stations 413 and 414, any damage and yielding were minimized. Thickness measurements made in this area using a calibrated computerized video measurement system[8] directly viewing the fracture face, ranged from 0.03415 inch to 0.03497 inch averaging 0.03476 inch. The engineering drawing specified a 0.040 +/-.003 inch thickness in the pocket.

[8] Smartscope by OGP (Optical Gaging Products)

X-ray fluorescence spectroscopy[9] on the interior surface (primer stripped) in the pocket area identified a spectrum consistent with 2024 aluminum alloy, as specified. Hardness tests and measurements of electrical conductivity were consistent with the specified temper condition, T-3[10]. Cross sections confirmed the appropriate thickness of cladding[11] on the exterior of the panel and at unmilled locations on the interior. Surface roughness measurements[12] on the chem-milled and stripped areas of the forward and aft fuselage bays averaged R_a 88 µ-inch in the aft bay and R_a 82 µ-inch in the aft bay. Boeing process specification BAC 5772[13] requires a R_a 63 µ-inch or finer finish on Type II components such as the crown skin and R_a 160 µ-inch or finer for Type I parts. No indications of blending of the chem-milled surface were noted at any of the stripped locations.

After removal of the sealant but with the primer intact, magnified visual examinations of the panel interior uncovered what appeared to be a smooth depressed line immediately adjacent to the intact chem-mill steps, as shown in figure 8. Visually the depressed line was apparent around each pocket on the removed panel including the received S-3L portion of the S-3L to S-2L fuselage bays.

Several metallographic cross sections were prepared through the chem-mill steps at different locations around the fuselage bays including at stringer and tear strap locations. The sections revealed a pattern around each chem-mill pocket. On the S-4L sides of each pocket, thinning of the pocket material was noted immediately adjacent to the fillet. For the chemical milling process, this type of thinning, at this location is generally referred to as channeling[14]. On the S-3L sides of each bay locally thicker regions were present adjacent to the fillets. This type of geometric feature is generally referred to as ridging[15]. Typical profiles illustrating channeling and ridging found on opposite sides of the aft fuselage bay at BS 429 are displayed in figure 9. The sides of each pocket (along the tear straps) also followed consistent patterns in the fillet area. Channeling was noted for most of their lengths, changing to ridging for the last few inches. This pattern was exhibited by all of the fuselage bays in the removed portion of the crown skin. Fillets with channeling or ridging could be optically identified under laboratory conditions using moderate stereomicroscope magnifications and oblique lighting.

Both the AMS and Boeing specifications[16] for chemical milling illustrate channeling and ridging as possible geometric features produced by the chemical milling process. Both specifications noted that neither feature is rejectable unless an associated dimension exceeds drawing requirements for that part. The drawing specified 0.062 inch (nominal) thick material prior to chemical milling. In the pockets the thickness was to be reduced to 0.040 inch +/-0.003 thick by the chemical milling process.

[9] Using a Thermo Scientific Niton XL3t-980 hand held x-ray fluorescence analyzer.
[10] Solution treated and naturally aged to a substantially stable condition.
[11] As specified in Federal specification QQ-A-250/F, 2 ½ % of nominal thickness per side.
[12] Using a Mitutoyo Surftest 402 with a 5µm stylus tip
[13] BAC 5772 “Chemical Milling Aluminum Alloys” rev W 13-May-2005
[14] Aerospace Material Specification AMS-C-81769, Chemical Milling of Metals, May 2008
[15] Ibid.
[16] AMS-C-81769 and Boeing BAC 5772

Dimensional measurements[17] on the removed sections found the minimum skin thickness at the channeling locations to be consistently less than the 0.037 inch minimum specified for the pockets. The thinnest section was 0.03486 inch at BS 387.5. At the locations showing ridging, the minimum section thickness was slightly greater than the maximum specified pocket thickness of 0.043 inch with the ridges showing greater thicknesses. The table below lists the minimum section thickness at each location and other dimensions. The listed pocket thicknesses were measured at the furthest points away from fillets in the individual sections (0.75 to 1.25 inch) and may not define a minimum thickness for the full pocket.

Ultrasonic thickness measurements[18] were made at some locations on the aircraft prior to the removal of the section. The central regions of the pockets were all indicated to be greater than the specified minimum thickness of 0.037 inch. Thickness measurements were also made on the aircraft across chem-mill steps at various locations with the minimum thickness recorded at each location. Additional measurements were later made in the laboratory on the removed section.

The metallographic sections were taken at or in close proximity to locations where the minimum section thickness had been previously measured ultrasonically, as listed in the table. At all locations of channeling, the ultrasonic measurements consistently overestimated the minimum section thickness. At locations of ridging, the ultrasonic measurements underestimated the minimum thickness.

Location	Minimum Thickness Section	Ridge Thickness Section	Full Thickness Section	Pocket Thickness Section	Ultrasonic Minimum Thickness
BS387.5 S-4L	.03486		.06177	.0429	.038
BS 398 S-4L	.03535		.06256	.0426	.038
BS 428.5 S-4L*	.03497		.06192	.0419	
BS 429 S-4L	.03626		.06283	.0437	.038
BS 429 S-3L	.04307	.04571	.06205	.040	.041-.040
BS432.5 S-3L	.04370	.04665	.06354	.040	.041-.040
BS 439 S-4L Radius	.03634		.06345	.04275	.038
BS 439 Tear Strap	.03693		.06311	.04212	.039
* **Section cut and measured by Boeing**					

With the primer intact, the through crack (between BS 386 and 387) was clearly visible at low magnifications on the inner surface. At higher magnifications a portion of the crack indication at BS 384 was visible as cracking in the primer as shown in figure 10. With the primer removed a smaller portion of the crack indication could be discerned at high optical magnifications with oblique lighting.

[17] Using a computerized video measurement system, Smartscope by OGP (Optical Gaging Products)
[18] IAW Boeing 757 Nondestructive Test Manual Part 4, Jan 15/2007.

On the internal surface of the panel, the through crack was apparent from approximately BS 385.5 to BS 387. To open the through crack, the panel was saw cut from the lower edge of the lap joint to the visible ends of the crack and the created tab separated with little or no force. Visual magnified examinations of the exposed crack surfaces revealed surfaces consistent with fatigue cracking from multiple origins on the interior surface. The initiation and propagation of the fatigue crack was visually very similar to the flap at the middle bay.

The adjacent chem-mill step areas of the forward bay were stripped of paint and visually inspected. Except at the previously noted eddy current crack indication, no cracking was visible at magnifications up to 50X. However, when the panel was cut and bent outward and fractured many additional areas of fatigue were noted propagating away from the interior surface, similar to the flap region in the middle bay. Including the through crack and the eddy current indication, fatigue was visible from about BS 381 to about BS 391.5. For most of the forward bay, the fatigue penetration was less than about 0.009 inches as shown in the upper view of figure 12. However, in the eddy current indication location, the fatigue penetration was up to 0.017 inch for a length of approximately 0.15 inch as shown in the lower view of figure 12. Measurements of relative penetration of the skin by fatigue measured at ½ inch body stations are depicted in figure 13. It should be noted that the deepest penetration noted above fell between the measurements point and is not reflected in the graph.

The previously mentioned metallographic sections taken for thickness measurements included one at BS 387.5 in the forward bay. The location was just aft of the through crack. Close inspection of the section revealed two 0.008 inch deep cracks in the thinnest section, as shown in figure 14.

No cracks were initially detected in the aft bay, by either eddy current or visual inspections. The bay was cut in half (about BS 428.5) and the forward portion was temporarily released to Boeing as a test piece for NDI procedures. Upon receipt Boeing stripped the paint from the chem-mill step areas and performed a fluorescent penetrant inspection (FPI). The FPI revealed a series of cracks along the chem-mill step at the lap joint. The indications extended from about BS 421.5 to the cut at BS 428.5. Subsequent FPI of the aft portion also uncovered crack indications extending aft another 1inch, to about BS 429.5. A cross section at about BS 428.5 confirmed the indications by revealing 2 parallel 0.007 inch deep cracks at the minimum section thickness similar to that shown in figure 14.

Portions of the flapped area, the through crack and the opened eddy current crack indication were examined with a scanning electron microscope (SEM). The SEM examinations confirmed the optical findings of multiple fatigue cracks initiating at the interior surface and propagating directly though the thickness of the skin. A typical view of fatigue at a full penetration area is displayed in the upper view of figure 15. Typically, the individual fatigue cracks independently initiated at surface features (pits) resulting from the chemical milling process, as shown in the lower view of figure 15. The individual cracks propagated independently, in many instances at slightly off set planes, through between 1/3 and 1/2 of the thickness before merging into a common fatigue front. In most of the fatigue areas a

change in surface texture from relatively smooth to much rougher was apparent at about the merge area. Fatigue striations were typically visible throughout the fatigue regions, as typified in the upper view of figure 16. At regions of partial fatigue penetration the fatigue terminus was sharply delineated as shown in the lower view of figure 16.

Through the thickness measurements of fatigue striation spacing were taken along 5 lines in the flap area, at body stations 411.8, 412.0, 412.5, 413.0 and 413.5, at 7 locations in the through crack, BS 385.8, 386.0, 386.2,386.5, 386.7, 386.9 and at 387.0 and at 2 locations at the opened crack indication, BS 383.85 and 383.9. For the measurements, images of resolved striations were recorded along with their relative X-Y coordinates and that of the originating surface. The SEM stage and viewing was arranged such that the distance of the image from the origin surface (crack length) was determined by the Y axis alone. Average striation spacing, expressed in inches per striation (da/dN), was then established using consecutive striation in each field of view with appropriate corrections for viewing magnification. Tables summarizing the data at each location are presented below, identified by body stations. Images used in measuring the fatigue striation spacing are contained in Appendices A-N.

BS 411.8 Through Fatigue Flap Appendix A

Image	Crack Length (in)	Scaled Mag	Stria Count	Image Distance (in)	da/dN *(in/cycle)	da/dN (μ in/cycle)
origin	0.00000				0.00E+00	0.00
3351	0.00528	40640	8	1.40	4.29E-06	4.29
3350	0.00638	40640	5	0.65	3.20E-06	3.20
3349	0.00783	16764	20	2.20	6.55E-06	6.55
3348	0.00870	12700	23	3.12	1.07E-05	10.68
3347	0.00906	19812	37	3.77	5.14E-06	5.14
3346	0.01110	7303	24	4.79	2.73E-05	27.30
3345	0.01295	4445	8	1.35	3.80E-05	37.96
3344	0.01370	6858	6	1.41	3.43E-05	34.27
3342	0.01709	4318	9	2.29	5.89E-05	58.93
3343	0.01831	3810	14	3.46	6.49E-05	64.87
3341	0.02181	3683	7	1.04	4.03E-05	40.34

* da/dN calculated as Image Distance divided by Stria Count result divided by Scaled Mag. Result in inches per cycle.

BS 412.0 Through Fatigue Flap Appendix B

Image	Crack Length (in)	Scaled Mag	Stria Count	Image Distance (in)	da/dN (in/cycle)	da/dN (μ in/cycle)
origin	0.00000				0.00E+00	0.00
3307	0.00406	30480	7	1.33	6.21E-06	6.21
3305	0.00571	34290	15	1.99	3.86E-06	3.86
3303	0.00657	21844	17	1.93	5.18E-06	5.18
3302	0.00717	17526	22	2.62	6.78E-06	6.78
3301	0.00799	18034	17	2.89	9.41E-06	9.41
3300	0.01012	5080	21	2.40	2.25E-05	22.50
3299	0.01390	6604	10	2.73	4.13E-05	41.26
3298	0.01591	11938	9	2.48	2.30E-05	23.04
3297	0.01972	4128	7	1.38	4.76E-05	47.59
3296	0.02295	3175	8	1.55	6.10E-05	61.02
3295	0.02602	4699	4	0.70	3.72E-05	37.24

BS 412.5 Through Fatigue Flap Appendix C

Image	Crack Length (in)	Scaled Mag	Stria Count	Image Distance (in)	da/dN (in/cycle)	da/dN (μ in/cycle)
origin	0.00000				0.00E+00	0.00
3322	0.00406	41910	5	0.90	4.29E-06	4.29
3321	0.00429	39370	6	1.65	6.99E-06	6.99
3323	0.00520	38100	12	2.15	4.70E-06	4.70
3318	0.00807	35027	14	1.98	4.03E-06	4.03
3317	0.01008	28575	18	2.00	3.89E-06	3.89
3316	0.01236	24130	26	2.10	3.35E-06	3.35
3315	0.01421	19685	18	2.90	8.18E-06	8.18
3314	0.01772	8573	24	3.60	1.75E-05	17.50
3313	0.01870	11113	15	2.40	1.44E-05	14.40
3312	0.02441	8636	22	2.13	1.12E-05	11.18
3311	0.02748	5461	10	1.35	2.47E-05	24.72
3310	0.03016	4657	18	2.73	3.25E-05	32.51

BS 413.0 Through Fatigue Flap Appendix D

Image	Crack Length (in)	Scaled Mag	Stria Count	Image Distance (in)	da/dN (in/cycle)	da/dN (μ in/cycle)
origin	0.00000				0.00E+00	0.00
3288	0.00441	39380	9	2.10	5.93E-06	5.93
3285	0.00579	38465	10	1.30	3.38E-06	3.38
3284	0.00626	35607	11	1.21	3.09E-06	3.09
3283	0.00799	27564	15	2.13	5.14E-06	5.14
3282	0.00870	15607	36	3.50	6.22E-06	6.22
3281	0.01028	13171	8	1.08	1.02E-05	10.20
3280	0.01134	8674	16	2.02	1.46E-05	14.55
3278	0.01417	5098	11	1.54	2.75E-05	27.46
3277	0.01531	4033	11	1.62	3.65E-05	36.52
3275	0.01807	3445	8	1.38	4.99E-05	49.89
3274	0.01917	9131	8	1.53	2.09E-05	20.95
3273	0.02394	4469	9	1.73	4.29E-05	42.89
3272	0.02433	4111	8	1.06	3.22E-05	32.23

BS 413.5 Through Fatigue Flap Appendix E

Image	Crack Length (in)	Scaled Mag	Stria Count	Image Distance (in)	da/dN (in/cycle)	da/dN (μ in/cycle)
origin	0.00000				0	0
3338	0.00315	37253	15	1.98	3.53E-06	3.53
3335	0.00547	28575	9	1.00	3.89E-06	3.89
3334	0.00709	21590	11	2.28	9.58E-06	9.58
3333	0.00906	8890	25	4.10	1.84E-05	18.45
3332	0.01252	4149	16	1.98	2.98E-05	29.75
3330	0.01433	5080	14	2.83	3.97E-05	39.72
3331	0.01657	3937	14	2.28	4.13E-05	41.28
3329	0.01957	4572	6	1.30	4.74E-05	47.39
3328	0.02000	3493	10	1.65	4.72E-05	47.24
3327	0.02583	3175	5	1.55	9.76E-05	97.64

BS 385.8 Through Crack Appendix F

Image	Crack Length (in)	Scaled Mag	Stria Count	Image Distance (in)	da/dN (in/cycle)	da/dN (μ in/cycle)
origin	0.00000				0.00E+00	0.00
3218	0.00319	44450	5	1.20	5.40E-06	5.40
3219	0.00539	36830	3	1.19	1.08E-05	10.80
3220	0.00740	23495	8	1.55	8.25E-06	8.25
3194	0.01110	17780	9	1.70	1.06E-05	10.62
3193	0.01252	13589	7	1.27	1.34E-05	13.35
3221	0.01370	11113	10	1.83	1.64E-05	16.42
3222	0.01547	8255	10	1.74	2.11E-05	21.08
3192	0.01902	3810	7	1.14	4.27E-05	42.74
3223	0.02181	4953	15	2.18	2.93E-05	29.28
3191	0.02472	5398	8	1.30	3.01E-05	30.11

BS 386.0 Through Crack Appendix G

Image	Crack Length (in)	Scaled Mag	Stria Count	Image Distance (in)	da/dN (in/cycle)	da/dN (μ in/cycle)
origin	0.00000				0.00E+00	0.00
3140	0.00335	28575	5.66	0.88	5.41E-06	5.41
3138	0.00567	28575	7	1.55	7.75E-06	7.75
3137	0.00614	25400	9	1.05	4.59E-06	4.59
3145	0.00669	17780	11	1.03	5.24E-06	5.24
3134	0.00756	25400	7	0.73	4.08E-06	4.08
3144	0.00949	10160	14	1.43	1.00E-05	10.02
3132	0.01130	6350	11	0.85	1.22E-05	12.17
3131	0.01622	5715	5.5	0.64	2.03E-05	20.28
3143	0.01787	8255	8	0.93	1.40E-05	14.01
3130	0.02106	5715	6	1.10	3.21E-05	32.08
3142	0.02240	3175	7	1.05	4.72E-05	47.24
3129	0.02622	5715	5.5	1.30	4.14E-05	41.36
3141	0.02630	2858	8	1.10	4.81E-05	48.12
3127	0.02815	5398	8	1.31	3.03E-05	30.34
3126	0.02913	6033	9	1.85	3.41E-05	34.07

BS 386.2 Through Crack Appendix H

Image	Crack Length (in)	Scaled Mag	Stria Count	Image Distance (in)	da/dN (in/cycle)	da/dN (μ in/cycle)
origin	0.00000				0.00E+00	0.00
3202	0.00283	38100	6	1.08	4.70E-06	4.70
3201	0.00906	28575	7	0.99	4.94E-06	4.94
3199	0.01224	22225	10	1.40	6.30E-06	6.30
3198	0.01783	11430	7.5	0.94	1.09E-05	10.94
3206	0.02224	16256	10	1.80	1.11E-05	11.07
3197	0.02602	13653	11	2.05	1.37E-05	13.65
3203	0.02917	13018	9	2.03	1.73E-05	17.28

BS 386.5 Through Crack Appendix I

Image	Crack Length (in)	Scaled Mag	Stria Count	Image Distance (in)	da/dN (in/cycle)	da/dN (μ in/cycle)
origin	0.00000				0.00E+00	0.00
3160	0.00224	33867	8	1.20	4.43E-06	4.43
3158	0.00232	23283	6	0.78	5.55E-06	5.55
3156	0.00606	25400	6	0.58	3.77E-06	3.77
3155	0.00827	17145	7	0.65	5.42E-06	5.42
3154	0.01075	25400	11	1.15	4.12E-06	4.12
3153	0.01362	28575	7	0.98	4.87E-06	4.87
3152	0.01551	12065	11	0.90	6.78E-06	6.78
3151	0.01961	17145	9	0.70	4.54E-06	4.54
3150	0.02614	3598	8	0.45	1.56E-05	15.63
3149	0.02898	6033	9	0.83	1.52E-05	15.20
3147	0.03039	4763	10	0.80	1.68E-05	16.80

BS 386.7 Through Crack Appendix J

Image	Crack Length (in)	Scaled Mag	Stria Count	Image Distance (in)	da/dN (in/cycle)	da/dN (μ in/cycle)
origin	0.00000				0.00E+00	0.00
3214	0.00260	52070	7	1.15	3.16E-06	3.16
3213	0.00610	77470	7	1.13	2.08E-06	2.08
3212	0.01008	39370	26	2.88	2.81E-06	2.81
3211	0.01472	17780	7	1.68	1.35E-05	13.46
3210	0.01870	7303	10	1.71	2.34E-05	23.42
3209	0.02236	6350	10	2.10	3.31E-05	33.07
3208	0.02697	4763	9	1.63	3.79E-05	37.91

BS 386.9 Through Crack Appendix K

Image	Crack Length (in)	Scaled Mag	Stria Count	Image Distance (in)	da/dN (in/cycle)	da/dN (μ in/cycle)
origin	0.00000				0.00E+00	0.00
3177	0.00177	38100	5	0.65	3.41E-06	3.41
3176	0.00224	31750	3	0.33	3.41E-06	3.41
3174	0.00323	25400	6.5	0.85	5.15E-06	5.15
3173	0.00382	28575	7	1.05	5.25E-06	5.25
3171	0.00516	28575	6	0.56	3.28E-06	3.28
3172	0.00713	28575	8	0.98	4.27E-06	4.27
3170	0.00858	12065	10	0.68	5.59E-06	5.59
3169	0.01087	8255	10	1.19	1.44E-05	14.39
3168	0.01366	3175	8	0.90	3.54E-05	35.43
3179	0.01685	3175	11	1.38	3.94E-05	39.37
3167	0.01799	2858	7	0.75	3.75E-05	37.50
3166	0.02079	3175	7	0.85	3.82E-05	38.25
3180	0.02303	3493	7	1.25	5.11E-05	51.13
3165	0.02449	2032	5	0.88	8.61E-05	86.12

BS 387.0 Through Crack Appendix L

Image	Crack Length (in)	Scaled Mag	Stria Count	Image Distance (in)	da/dN (in/cycle)	da/dN (μ in/cycle)
origin	0.00000				0.00E+00	0.00
3225	0.00303	34925	8	0.83	2.95E-06	2.95
3187	0.00661	27305	11	3.00	9.99E-06	9.99
3215	0.00898	13653	9	1.75	1.42E-05	14.24
3185	0.01138	6033	9.33	1.09	1.94E-05	19.40
3216	0.01335	3429	10.5	1.49	4.13E-05	41.31
3183	0.01677	6350	9	1.78	3.11E-05	31.06
3182	0.02063	3175	7	1.45	6.52E-05	65.24

BS 383.85 Crack Indication Appendix M

Image	Crack Length (in)	Scaled Mag	Stria Count	Image Distance (in)	da/dN (in/cycle)	da/dN (μ in/cycle)
origin	0.00000				0.00E+00	0.00
3233	0.00386	39370	8	1.10	3.49E-06	3.49
3235	0.00516	44450	7	0.75	2.41E-06	2.41
3237	0.00772	45720	7	0.86	2.69E-06	2.69
3238	0.00850	53975	4	0.55	2.55E-06	2.55
3239	0.01110	34290	9	0.79	2.55E-06	2.55
3242	0.01303	22860	9.5	0.90	4.14E-06	4.14
3243	0.01642	27940	8	0.84	3.75E-06	3.75

BS 383.9 Crack Indication Appendix N

Image	Crack Length (in)	Scaled Mag	Stria Count	Image Distance (in)	da/dN (in/cycle)	da/dN (μ in/cycle)
origin	0.00000				0.00E+00	0.00
3369	0.00094	69850	7	1.79	3.66E-06	3.66
3366	0.00437	48260	8	1.53	3.95E-06	3.95
3365	0.00480	41275	5	1.00	4.85E-06	4.85
3364	0.00736	49530	15	1.64	2.21E-06	2.21
3363	0.00913	45720	7	0.73	2.28E-06	2.28
3362	0.00992	44450	5	0.58	2.59E-06	2.59
3361	0.01138	41275	9	1.88	5.06E-06	5.06
3359	0.01291	35560	6	0.80	3.75E-06	3.75
3358	0.01417	33020	9	1.51	5.08E-06	5.08
3357	0.01516	28575	8	1.25	5.47E-06	5.47
3356	0.01657	20066	11	1.40	6.34E-06	6.34

Joe Epperson
Senior Metallurgist

Figure 1—Skin flap location indicated by red arrow in upper view showing its relative location to the cockpit and the passenger entry door (L1). Lower view shows closer side view of the skin flap and resulting hole.

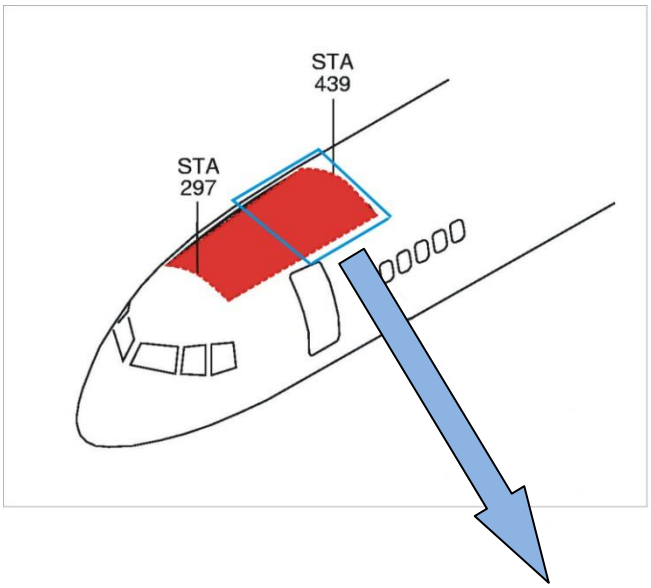

Figure 2—Illustration showing the location of the crown skin (in red) on the aircraft at left and some of the details of construction for the aft portion of the panel below. Fuselage bays containing the visible crack, the flap and crack indications are noted

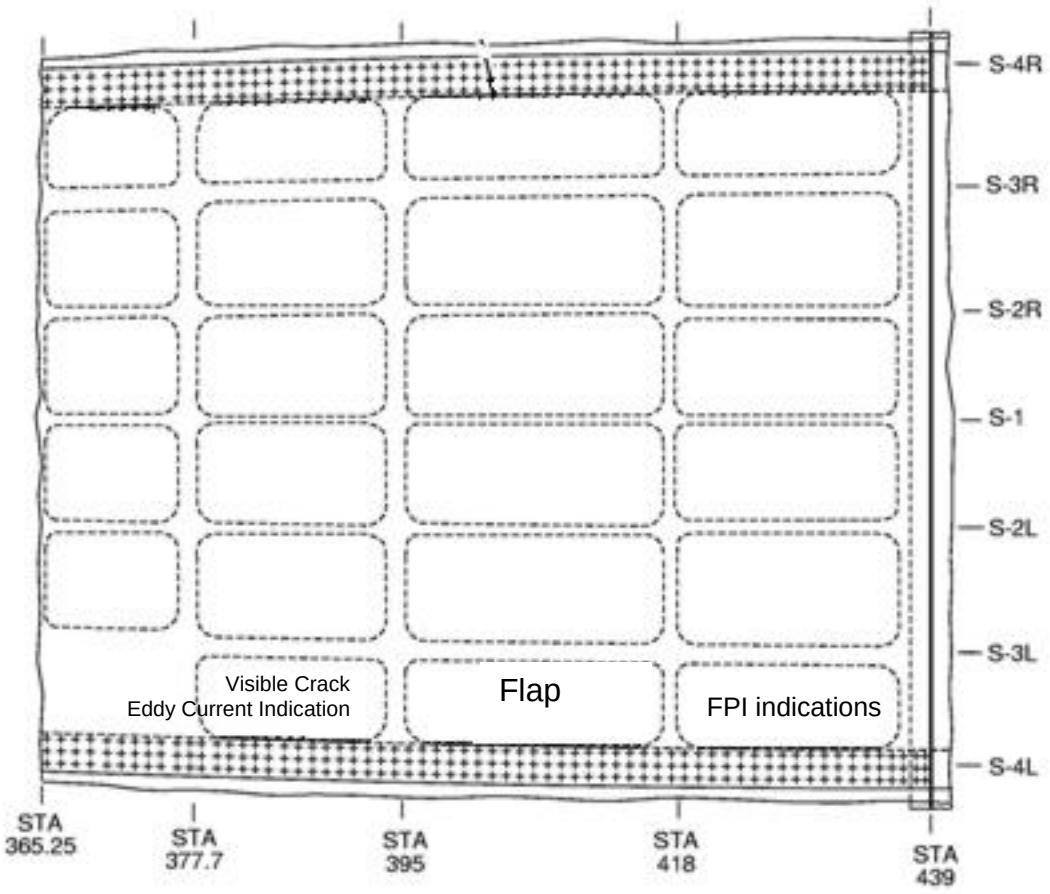

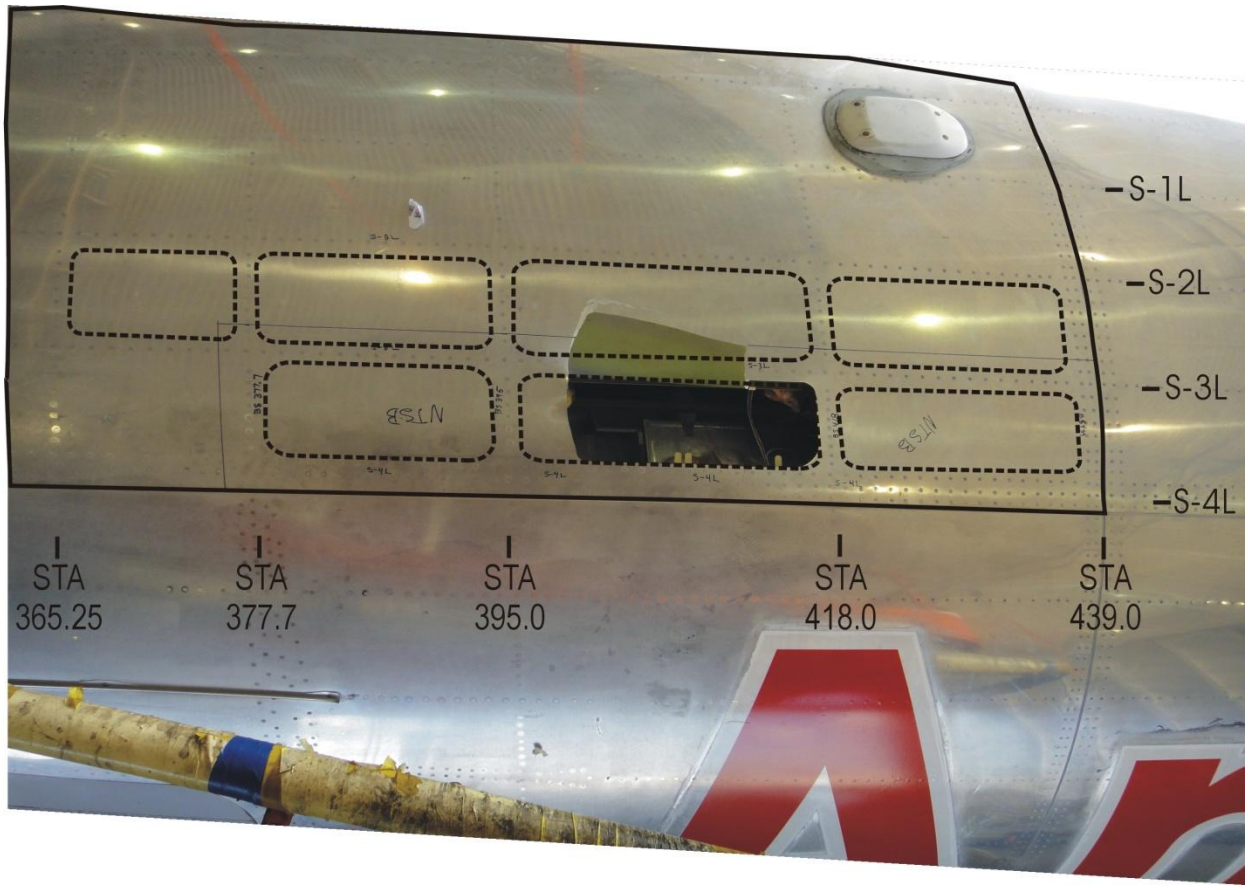

Figure 3—An overhead view of the skin flap and resulting hole and surrounding area with body station and stringers noted. Dashed lines denote the approximate location and shapes of the internal chemically milled pockets.

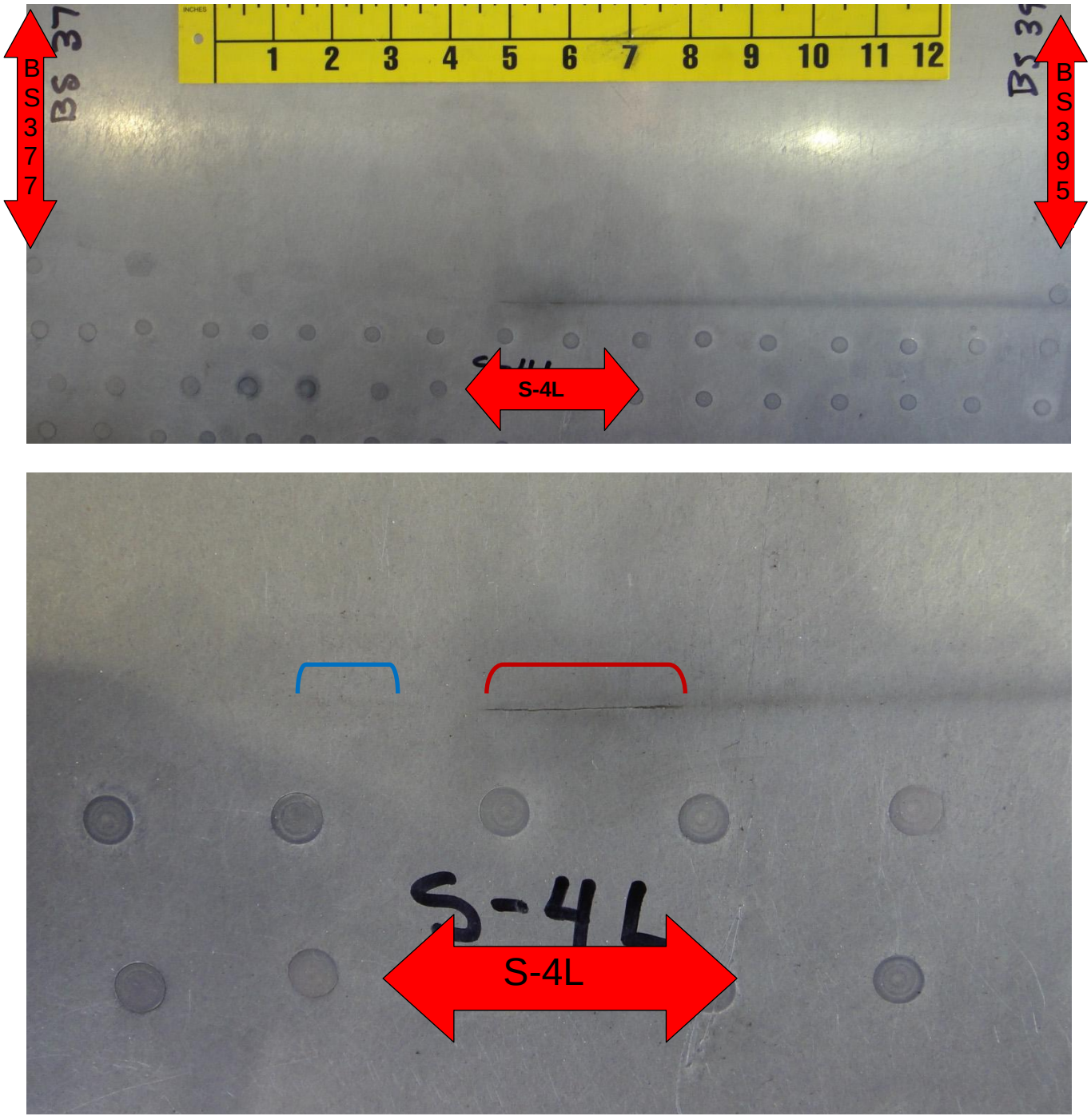

Figure 4—Closer views of the exterior surface of the forward bay showing the thru crack and trailing dark deposits (top) and at bottom the relative locations of the through crack (red bracket) and the eddy current crack indication (blue bracket).

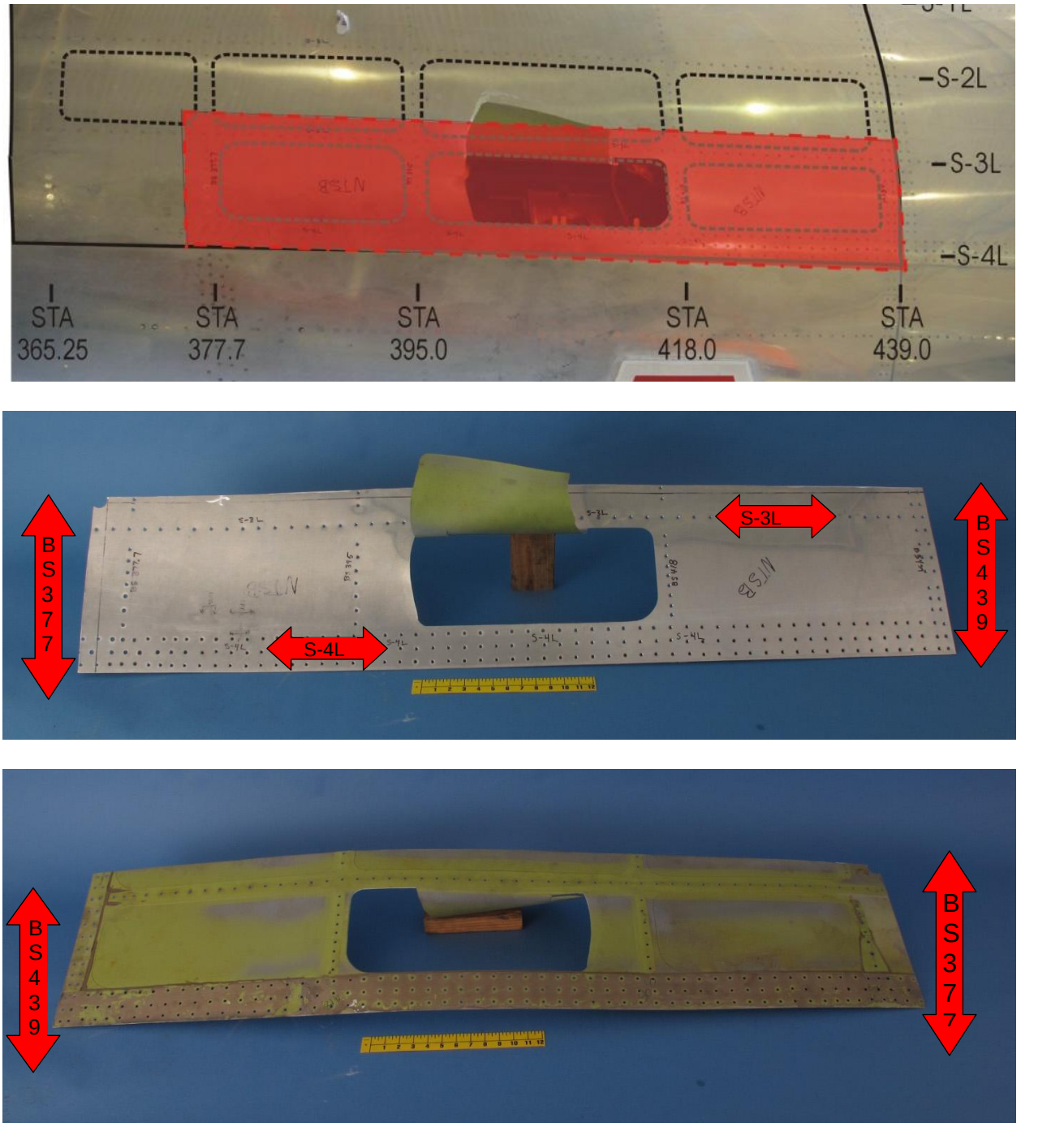

Figure 5—Upper view illustrates the area of the crown skin removed with a shaded red box. Lower views show the exterior and interior surface of the as-removed panel section.

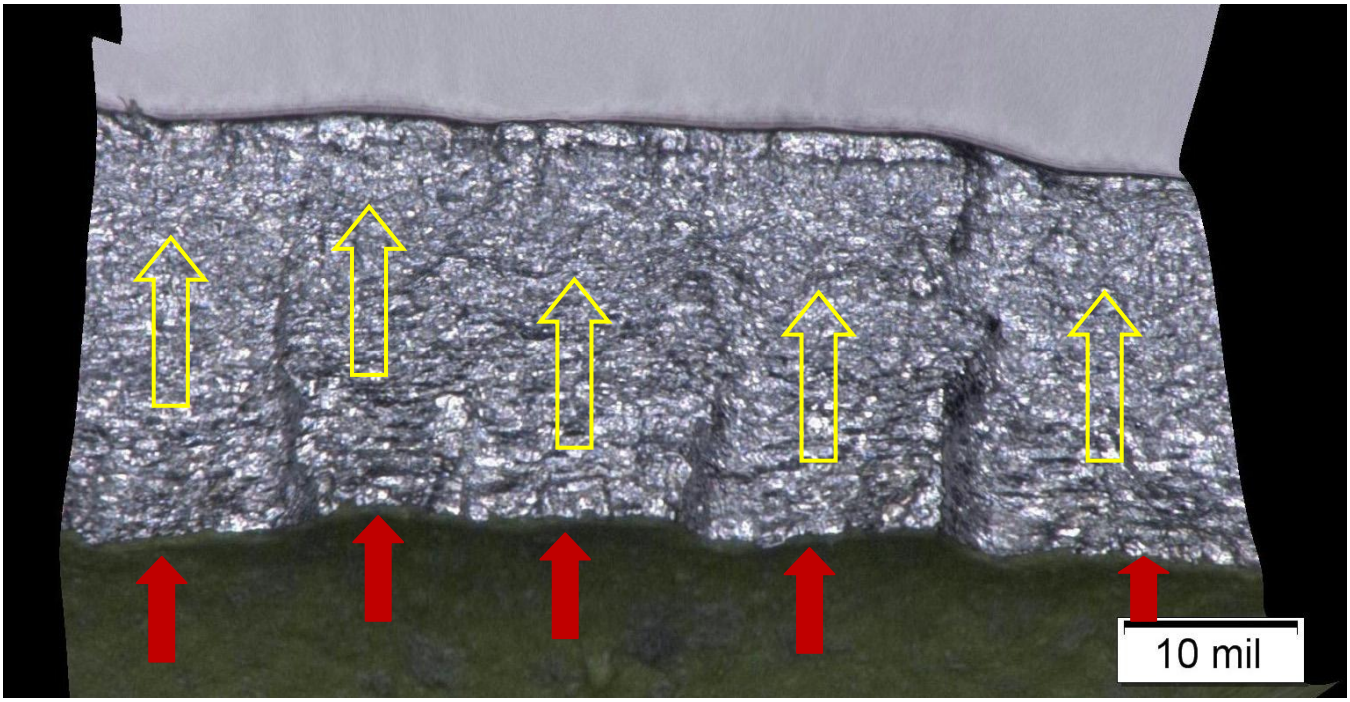

Figure 6—An area of fatigue showing typical multiple offset initiation points (red arrows) on the interior surface with progression (yellow arrows) outward through the thickness of the skin. Chart below plots the amount of fatigue as a percentage of total skin thickness along the edge of the hole. Image is a digital 3-D reconstruction.

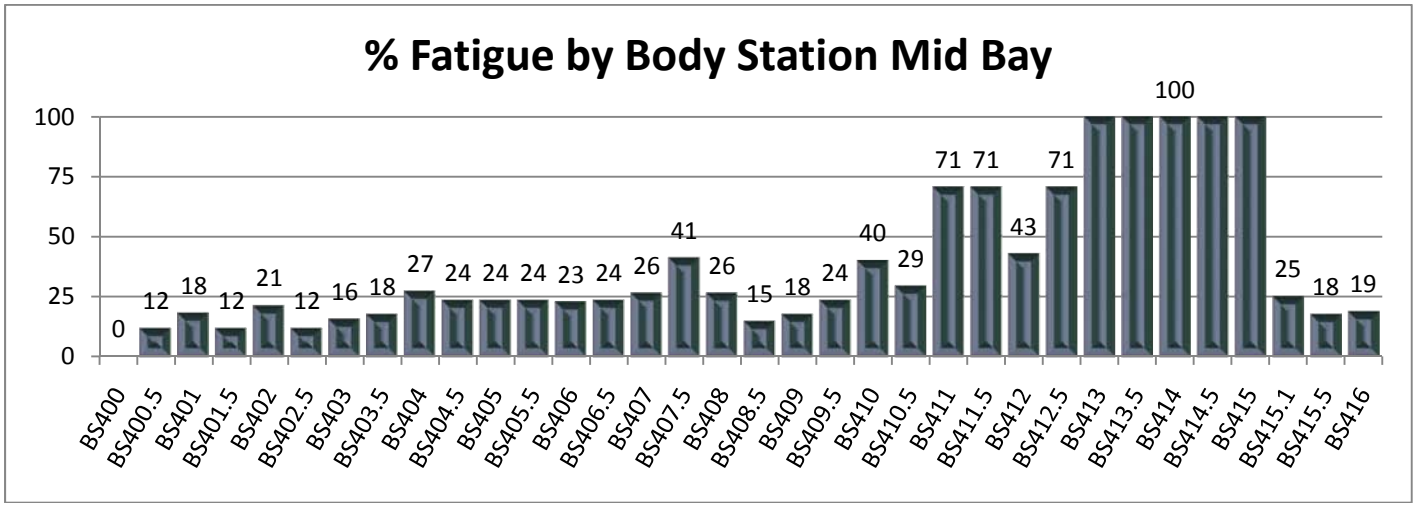

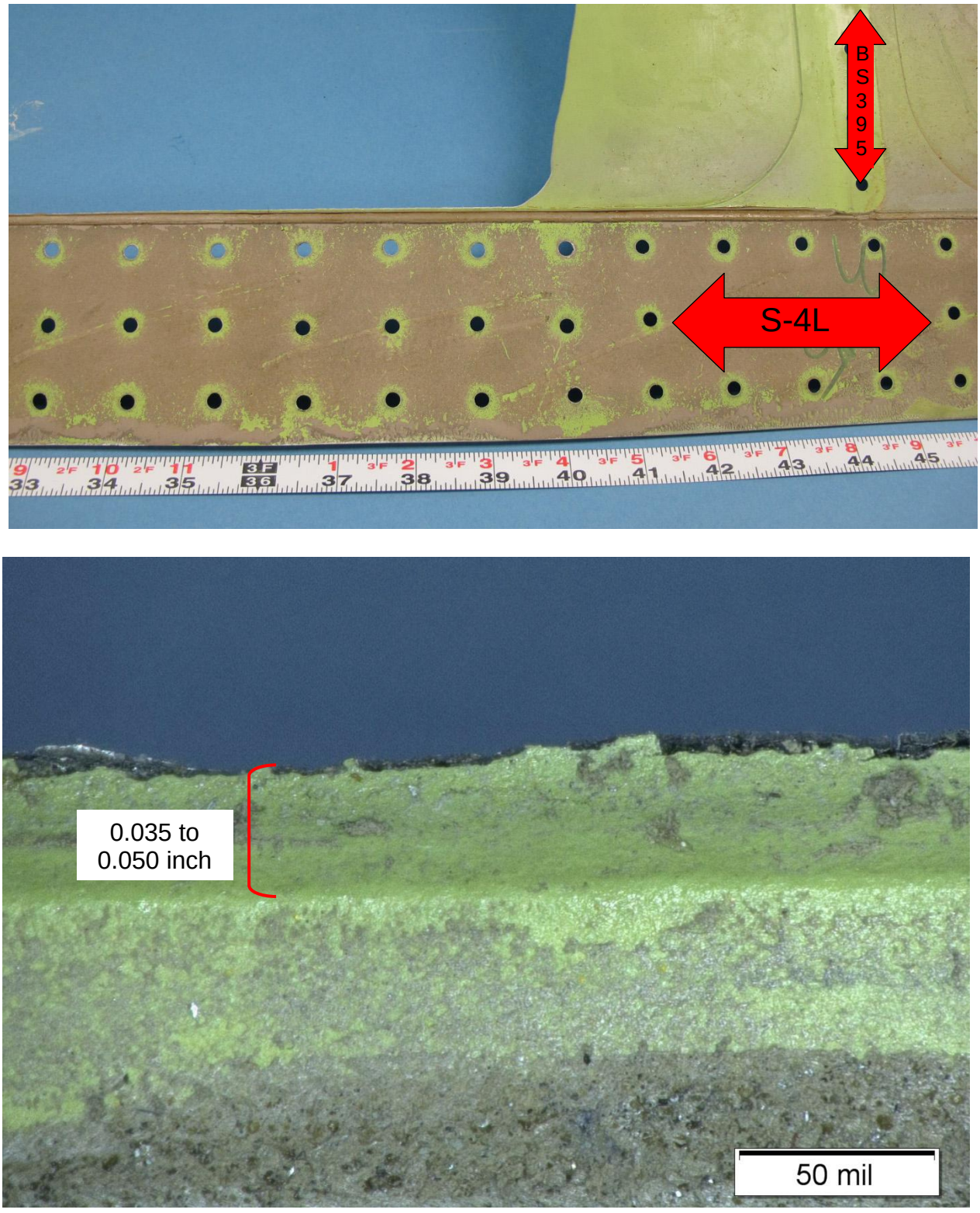

Figure 7—The upper image shows the relationship of the flap to the chem-mill step at stringer 4L and the partial obscuration of the step by the sealant (brown). Lower view shows a close up view of the chem-mill step (bracket) after the sealant was removed.

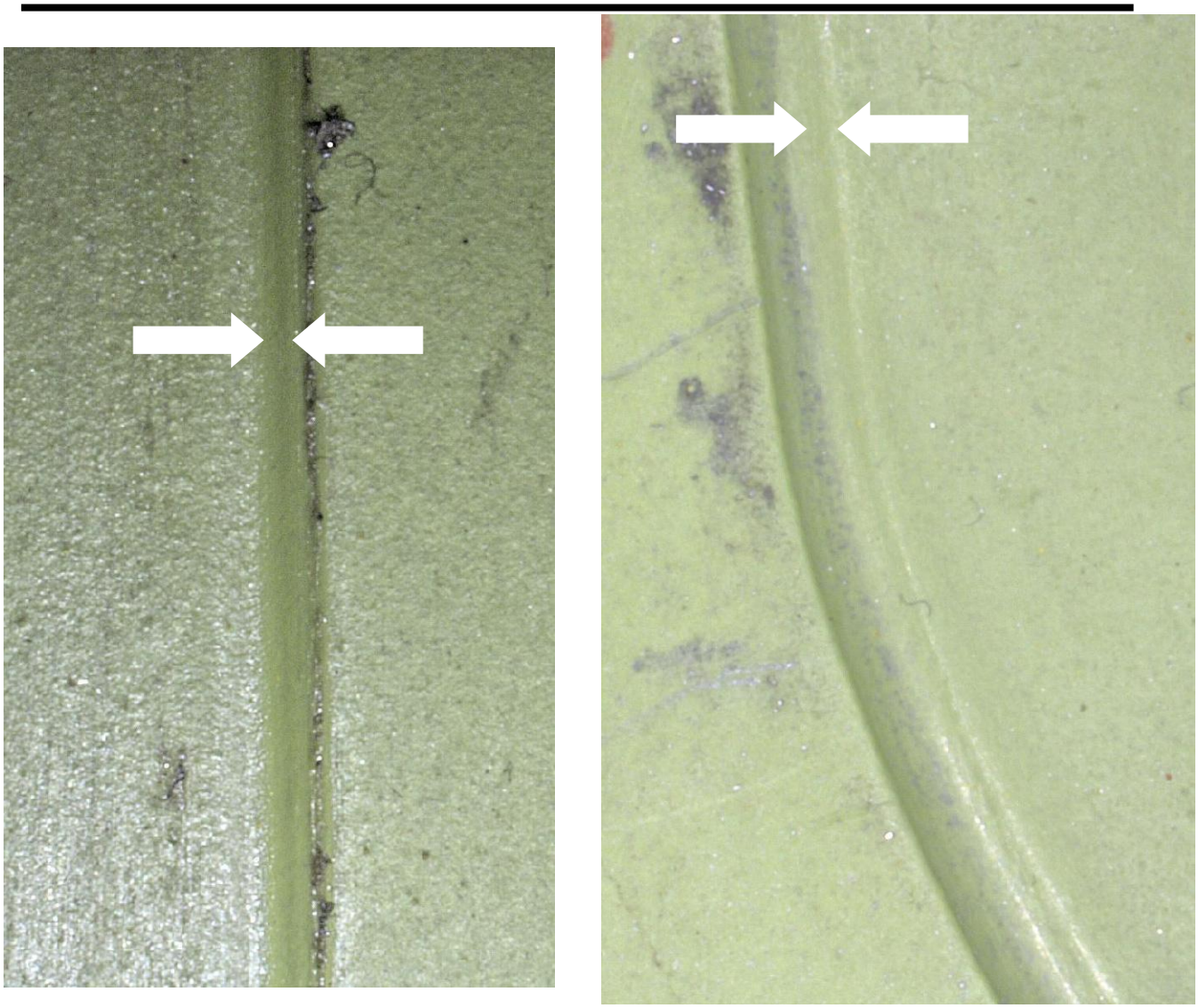

Figure 8—Views depicting the visually depressed line (between arrows) at the chem-mill step.

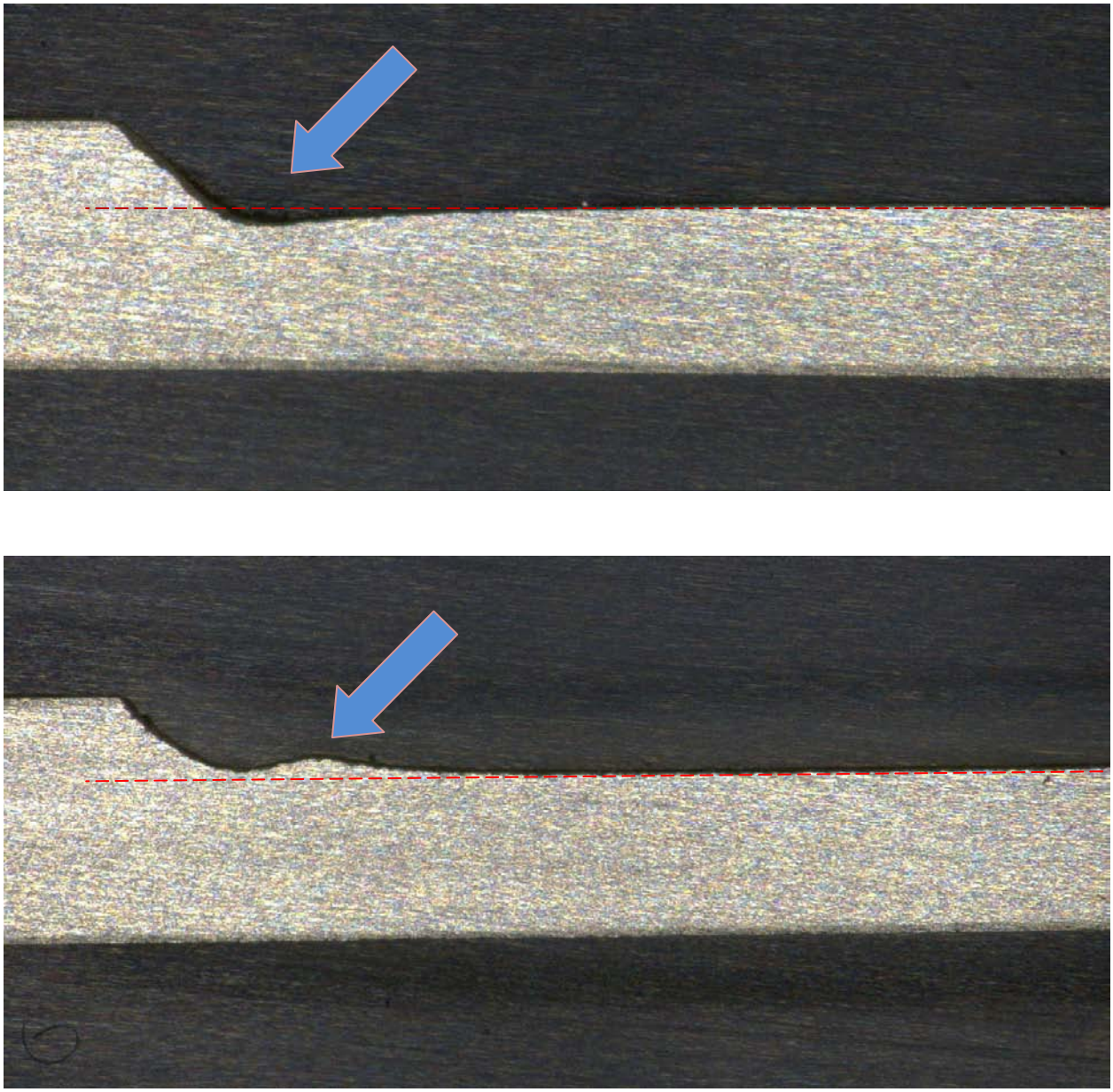

Figure 9—Cross sections through the chem-mill steps at BS 429. Upper profile shows channeling (arrow) at the lap joint step. Lower view shows ridging at the S-3L pad step. Dashed red lines are approximate projections of the average surface of the pocket.

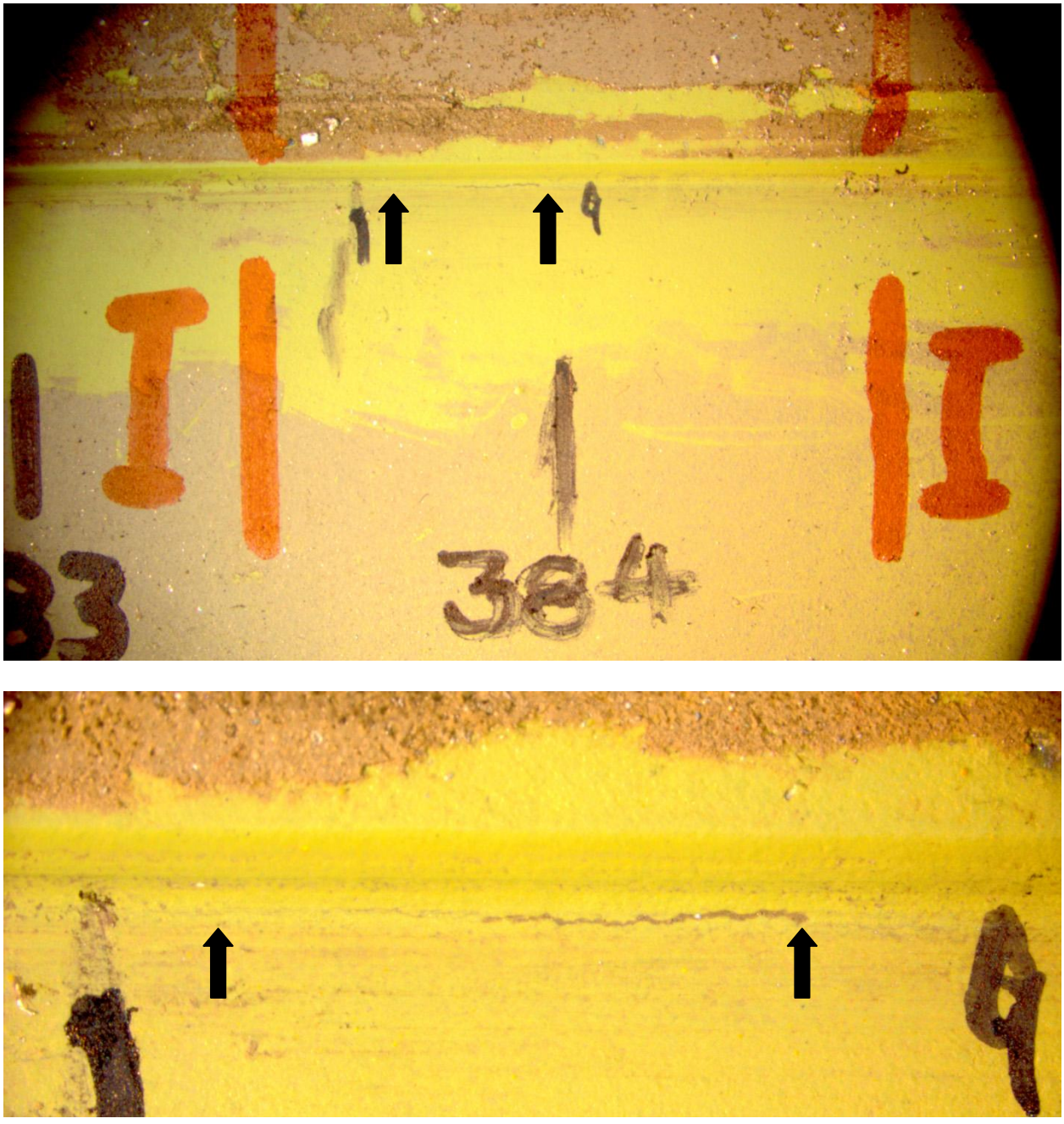

Figure 10—Views of the interior surface of the forward bay at the eddy current crack indication at BS 384. Red “I” marks indicate approximate eddy current size of indication. Black arrows indicate the visible portion through the primer. Higher magnification view of the visual crack shown in the lower view.

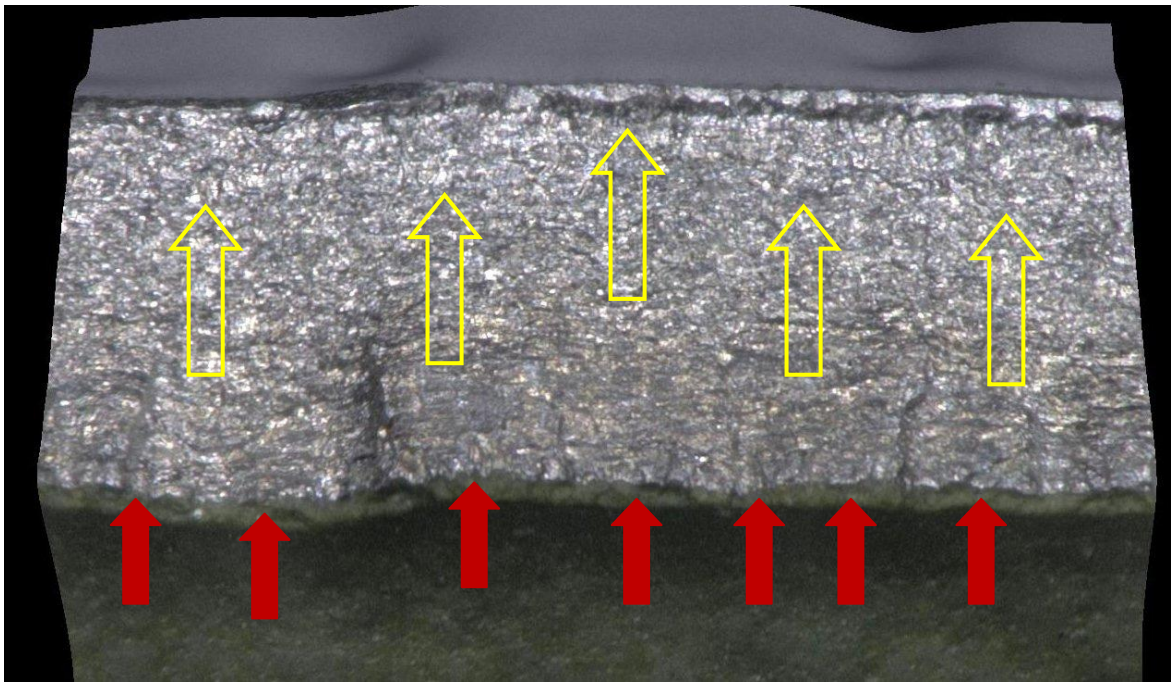

Figure 11—A typical portion of the opened through crack showing multiple initiation points (red arrows) on the interior surface with propagation (yellow arrows) through the thickness of the skin. Image is a digital 3-D reconstruction. Approximate 150x Mag

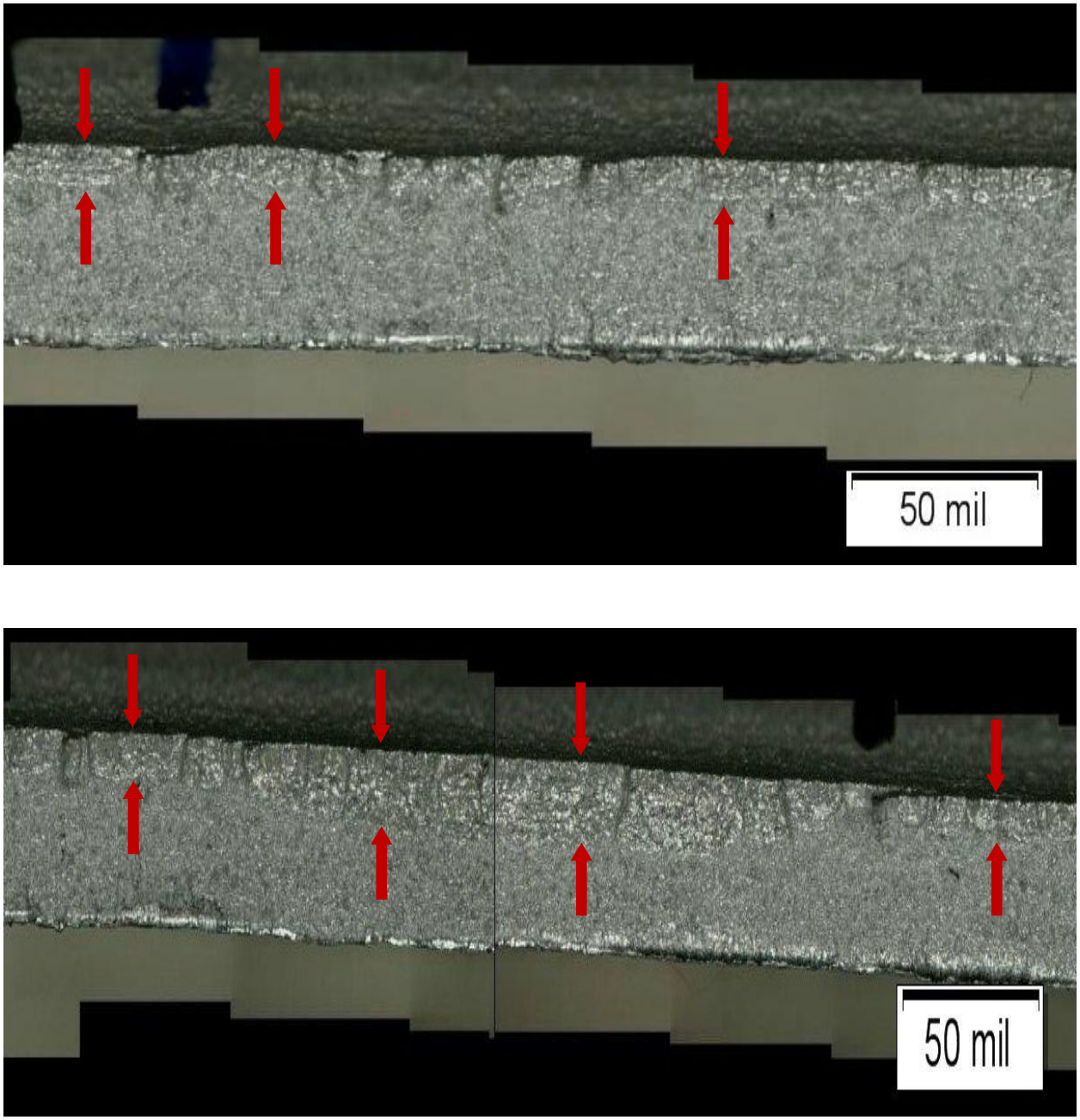

Figure 12—Upper view shows a typical portion of the opened crack in the forward bay with the fatigue regions, between red arrows. Interior surface and chem-mill step at top. Lower view shows the eddy current crack indication area. Both images are stitched mosaics. The upper image has been stretched 50% vertically and the lower image has been vertically stretched 100% to better show the fatigue.

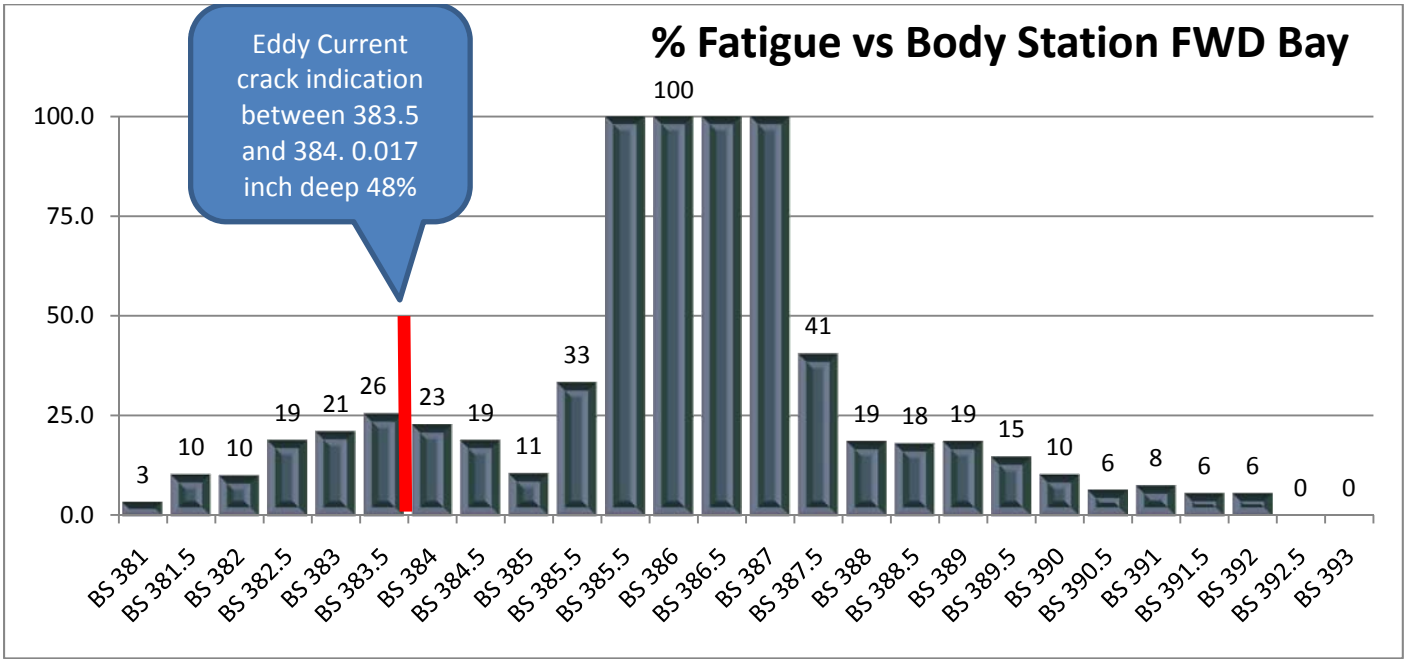

Figure 13—Graph showing the relative amount of fatigue penetration as a percentage of skin thickness in the forward bay. Measurements approximately every ½ inch. Note that the eddy current indication fell between measurement points.

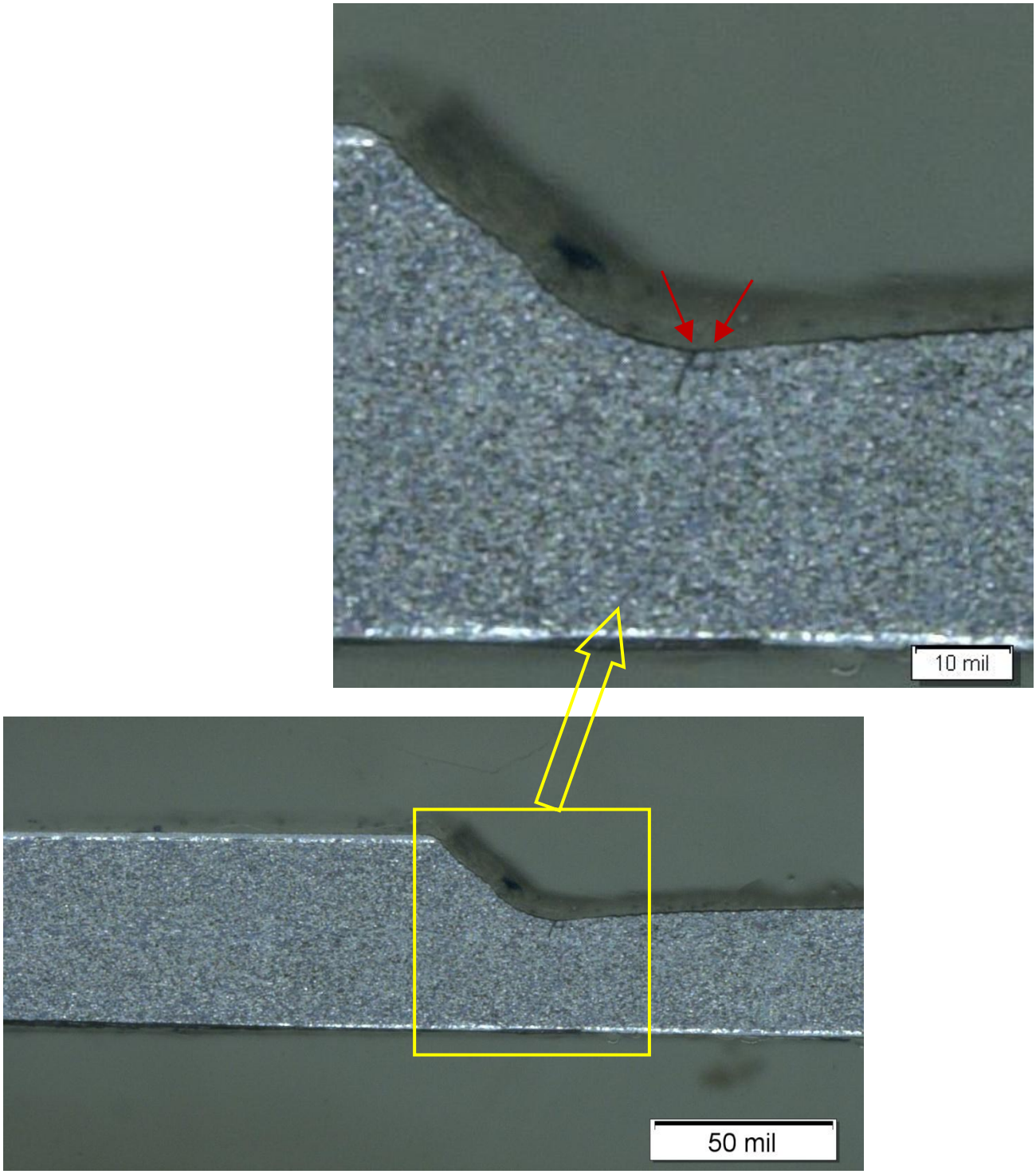

Figure 14—Images of cracking (arrows) in channel of lap joint chem-mill step at BS 387.5. Cracks measured 0.008 inch deep.

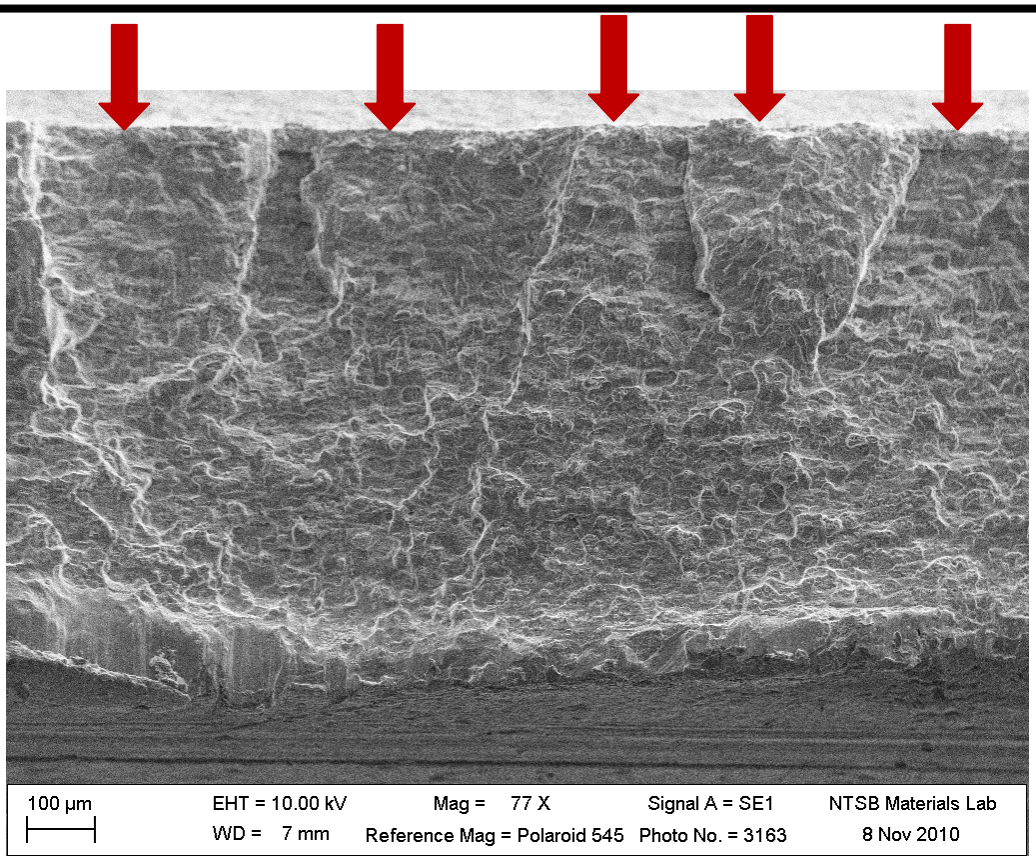

Figure 15—A typical area of full thickness fatigue (BS 836.9) is displayed in the upper view showing multiple fatigue origins (red arrows) at the interior surface (top in both views). Many of the origins were at surface pits from the chemical milling process as shown at BS 412.5 in the lower view.

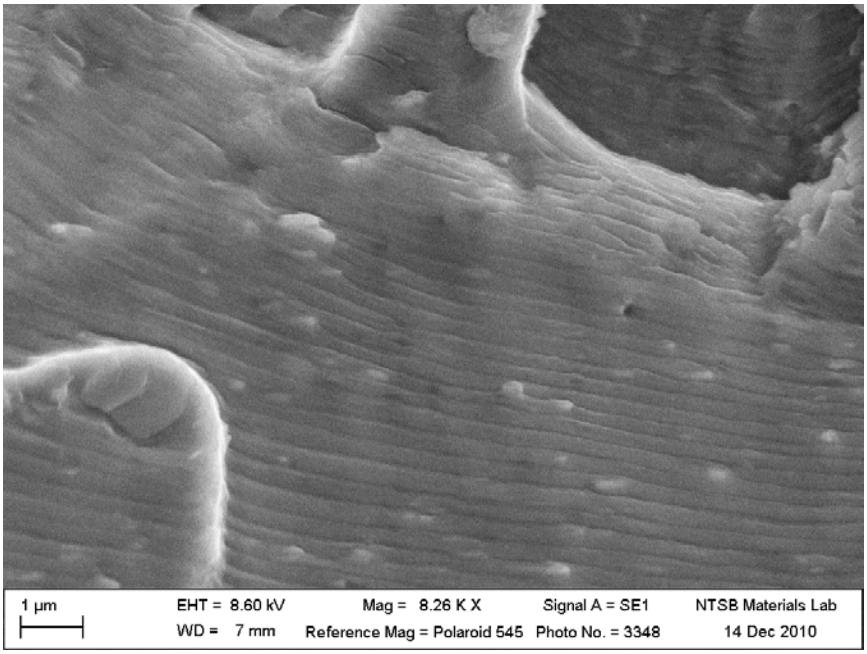

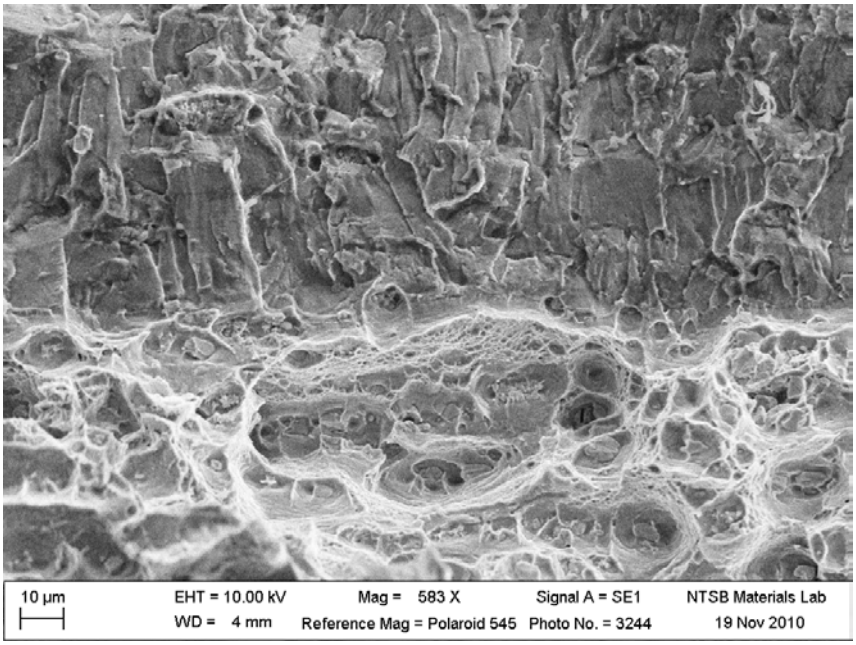

Figure 16—Top view shows typical striations found in fatigue areas. Lower view shows a typical fatigue terminus in the partial fatigue penetration regions. Fatigue is propagating from the image top to the bottom in both views.